Title

Heptavalent Neptunium in a Gas-Phase Complex: (NpVIIO3 +)(NO3 —)2

Journal

Inorganic Chemistry, 55(19)

ISSN

0020-1669

Authors

Dau, Phuong D

Maurice, Rémi

Renault, Eric

et al.

Publication Date

2016-10-03

DOI

10.1021/acs.inorgchem.6b01617

Heptavalent Neptunium in a Gas-Phase Complex: $(Np^{VII}O_3^+)(NO_3^-)_2$

Phuong D. Dau[a], Rémi Maurice[b,*], Eric Renault[c], John K. Gibson[a,*]

[a] *Chemical Sciences Division, Lawrence Berkeley National Laboratory, Berkeley, California 94720, USA*

[b] *SUBATECH, UMR CNRS 6457, IN2P3/EMN Nantes/Université de Nantes, 4 rue Alfred Kastler, BP 20722, 44307 Nantes Cedex 3, France*

[c] *CEISAM, UMR CNRS 6230, Université de Nantes, 2 rue de la Houssinière, BP 92208, 44322 Nantes Cedex 3, France*

*Corresponding authors: remi.maurice@subatech.in2p3.fr; jkgibson@lbl.gov

Abstract

A central goal of chemistry is to achieve ultimate oxidation states, including in gas-phase complexes with no condensed phase perturbation. In the case of the actinide elements the highest established oxidation states are labile Pu(VII) and somewhat more stable Np(VII). We have synthesized and characterized gas-phase $AnO_3(NO_3)_2^-$ complexes for An = U, Np and Pu by endothermic NO_2 elimination from $AnO_2(NO_3)_3^-$. It was previously demonstrated that the PuO_3^+ core of $PuO_3(NO_3)_2^-$ has a Pu-O$^\bullet$ radical bond such that the oxidation state is Pu(VI); it follows that in $UO_3(NO_3)_2^-$ it is the stable U(VI) oxidation state. Based on the relatively more facile synthesis of $NpO_3(NO_3)_2^-$, a Np(VII) oxidation state is inferred. This interpretation is substantiated by reactivity of the three complexes: NO_2 spontaneously adds to $UO_3(NO_3)_2^-$ and $PuO_3(NO_3)_2^-$, but not to $NpO_3(NO_3)_2^-$. This unreactive character is attributed to a $Np(VII)O_3^+$ core with three stable Np=O bonds, this in contrast to reactive U-O$^\bullet$ and Pu-O$^\bullet$ radical bonds. The computed structures and reaction energies for the three $AnO_3(NO_3)_2^-$ support the conclusion that the oxidation states are U(VI), Np(VII) and Pu(VI). The results establish the extreme Np(VII) oxidation state in a gas phase complex, and demonstrate the inherently greater stability of Np(VII) versus Pu(VII).

Introduction

A core attribute of the chemistry of the early actinide (An) elements is the accessibility of multiple oxidation states under moderate conditions, notably An(III/IV/V/VI) for An = U, Np and Pu. Whereas the highest accessible uranium oxidation state is U(VI), Np(VII) and Pu(VII) exist transiently in alkaline solutions, as reported nearly half a century ago by Spitsyn et al.[1] Both Np(VII) and Pu(VII) in aqueous solutions have been confirmed, with species such as $NpO_2(OH)_4^-{}_{aq}$ and $AnO_4(OH)_2^{3-}{}_{aq}$ (An = Np, Pu) having been proposed.[2-5] The lower stability of $Pu(VII)_{aq}$ versus $Np(VII)_{aq}$ is reflected in the standard reduction potentials, E^o(VII/VI), in alkaline solutions: 0.95 V for $PuO_4(OH)_2^{3-}$ and 0.58 V for $NpO_4(OH)_2^{3-}$.[6] Metastable Np(VII) has also been reported under acidic conditions.[7] Heptavalent Np and Pu have also been prepared in solid oxide compounds that contain a highly electropositive electron donor metal ion such as Li^+ or Na^+. The first such compound was Li_5NpO_6 reported by Keller and Seiffert in 1969.[8] Other compounds include $LiCo(NH_3)_6NpO_8(OH)_2$,[9] $Na_4AnO_4(OH)_3$ (An = Np, Pu)[10] and Na_5NpO_6.[11]

In condensed phases, the highest oxidation states are generally stabilized by the coordination environment, such as by hydroxyl coordination in highly alkaline solutions and by alkali metal cations in solid oxides. The existence of high oxidation states in gas-phase complexes can provide an evaluation of their inherent stabilities in the absence of secondary stabilizing interactions. The relative simplicity of gas-phase species furthermore presents the opportunity to perform high-level quantum chemical calculations of electronic structures and bonding. The case of octavalent plutonium is an intriguing contemporary example. Interest in Pu(VIII) derives largely from the atomic ground state of Pu, $[Rn]5f^67s^2$; engagement of all eight valence electrons in bonding would result in the Pu(VIII) oxidation state, in analogy with closed-shell Os(VIII) in volatile OsO_4. The PuO_4 molecule containing Pu(VIII) has been inferred based on indirect effects, including an apparently high volatility of Pu during ozonation of alkaline solutions of Pu(VI).[12-14] However, quantum chemical calculations have rather convincingly demonstrated that in ground-state PuO_4 the oxidation state is actually Pu(V), and that the molecule can be represented as $(PuO_2)^+(O_2)^-$.[15] Subsequent calculations on $PuO_nF_{(8-2n)}$ molecules revealed that even with highly electronegative fluorine ligands, only metastable species having Pu(VIII) are viable.[16]

The ground atomic configuration of Np is $[Rn]5f^46d^17s^2$ such that chemical engagement of all valence electrons results in Np(VII), which is a well-established oxidation state in condensed phases. The stability of Np(VII) in the gas phase has received less attention than that of Pu(VIII) despite that condensed phase properties, such as the VII/VI reduction potentials, indicate that Np(VII) should be more accessible than Pu(VII), and even more so than Pu(VIII). As for gas-phase Pu(VIII), there have been only circumstantial indications of Np(VII) in the gas phase. In particular, $Np^{VII}F_7$ and $Np^{VII}O_3F$ have been proposed based on the volatility of Np in the presence of fluorinating and oxidizing atmospheres at high temperature.[17] However, there is no direct evidence for either species, nor for the Np(VII) oxidation state in the postulated molecules.

Collision induced dissociation (CID) elimination of NO_2 from gas-phase nitrate complexes is a facile route to achieving accessible higher oxidation states of metals, via the generic unimolecular decomposition reaction (1), where *N* is the initial oxidation state.[18-22]

$$M^{N}O_X(NO_3)_Y^{(N-2X-Y)} \rightarrow M^{N+1}O_{X+1}(NO_3)_{Y-1}^{(N-2X-Y)} + NO_2 \quad (1)$$

The increase in oxidation state indicated in reaction (1) occurs only if a higher oxidation state is adequately accessible such that an additional M=O double bond is formed. In the event that a higher oxidation state is not accessible, such as in $LaO(NO_3)_3^-$ from $La^{III}(NO_3)_4^-$, the resulting M-O$^\bullet$ radical bond is highly reactive. For example, $LaO(NO_3)_3^-$ exothermically abstracts a hydrogen atom from water to recover the stable La(III) oxidation state in $La(OH)(NO_3)_3^-$.[23]

In previous work, gas-phase CID unimolecular decomposition of a plutonyl nitrate anion complex was explored. Reaction (2), where An = Pu, was studied in an attempt to access the Pu(VII) oxidation state in the gas phase.[24]

$$An^{VI}O_2(NO_3)_3^- \rightarrow AnO_3(NO_3)_2^- + NO_2 \quad (2)$$

However, quantum chemical calculations revealed that the oxidation state in the $PuO_3(NO_3)_2^-$ product is not Pu(VII) but rather Pu(VI), and that a Pu-O$^\bullet$ (rather than a Pu=O) bond is created in reaction (2). In essence, it was concluded that a radical oxygen atom does not oxidize Pu(VI) to Pu(VII) in the PuO_3^+ core of the product complex, $(PuO_3^+)(NO_3^-)_2$. In the present work, this approach, specifically reaction (2), is extended to Np(VI) with a goal of achieving oxidation to yield a gas-phase Np(VII) complex and evaluate the intrinsic stability of Np(VII), particularly in comparison with that of Pu(VII). Gas-phase $AnO_3(NO_3)_2^-$ anion complexes were produced for An = U, Np and Pu, where uranium was included for comparison because the U(VII) oxidation state is chemically inaccessible such that the uranium complex provides a good basis for comparison. Association reactions of the three $AnO_3(NO_3)_2^-$ complexes with NO_2 to regenerate the $AnO_2(NO_3)_3^-$ were studied to evaluate their comparative stabilities and thereby deduce oxidation states. Quantum chemical calculations of the structures of the complexes and the reaction energetics substantiate the interpretations of the experimental observations.

Experimental Procedures

Caution! The Np-237 and Pu-242 isotopes employed in these experiments are highly radioactive and must be handled only with proper safety precautions.

The general experimental approach has been previously described.[24] Anionic actinyl tris-nitrate complexes, $AnO_2(NO_3)_3^-$ for An = Np and Pu, were produced by electrospray ionization (ESI) of ethanol solutions containing 100 μM AnO_2^{2+} (diluted from 28 mM $NpO_2(ClO_4)_2$ at pH = 1 and 8 mM $PuO_2(ClO_4)_2$ at pH = 1) and 500 μM HNO_3. For uranium, a 10 mM $UO_2(NO_3)_3^-$ stock solution (pH = 1) was diluted with ethanol to 100 μM for ESI. The U-238, Np-237 and Pu-242 isotopes are all radioactive and must be handled with proper controls.[25] The experiments were performed using an Agilent 6340 quadrupole ion trap mass spectrometer (QIT-MS) with a MS^n CID capability; for this instrument the CID energy is a parameter that provides an indication of relative ion excitation. Ions in the trap can also undergo low-energy ion-molecule reactions at ~300 K,[26] by introducing a reaction time of up to 10 s without applying a CID

voltage. Anion mass spectra were acquired using the following parameters: solution flow rate, 60 µL/h; nebulizer gas pressure, 12 psi; capillary voltage offset and current, -4000 V and 208 nA; end plate voltage offset and current, -500 V and 3025 nA ; dry gas flow rate, 3 l/min; dry gas temperature, 325 °C; capillary exit, -50.0 V; skimmer, -36.3 V; octopole 1 and 2 DC, -10.9 V and -3.0 V; octopole RF amplitude, 190 Vpp; lens 1 and 2, 10.0 V and 91.0 V; trap drive, 50.0. Nitrogen gas for nebulization and drying was supplied from the boil-off of a liquid nitrogen Dewar. The background water pressure in the ion trap is estimated as ~10^{-6} Torr;[27] reproducibility of hydration rates of $UO_2(OH)^+$ [28] established that the water pressure was constant to within less than 10%. The helium buffer gas pressure in the trap is constant at ~10^{-4} Torr.

The ion trap has been modified to allow for the introduction of reagent gases through a gas-handling manifold and a leak valve.[25] While NO_2 gas (≥99.5%, Sigma Aldrich) was directly introduced into the ion trap, the liquid toluene-d8 reagent (99.6%, Cambridge Isotope Laboratory) in a reservoir was degassed by repeated freeze-vacuum-thaw cycles prior to introducing the vapor into the QIT. The pressures of NO_2 and toluene-d8 were not known, but were estimated to be in the range of 10^{-6} to 10^{-5} Torr based on the change in pressure indicated by an ion gauge external to the ion trap. For a given reagent gas the experiments were carried out using essentially constant reagent pressures (to within less than 10%), which allows for direct comparison of reactivity results.

Computational Details

We follow the same computational procedure as the one we previously applied on plutonium nitrate complexes[24] for the sake of comparing the data at the same, established level of theory. Therefore, for the $PuO_2(NO_3)_3^-$ and $PuO_3(NO_3)_2^-$ systems, the same geometrical and electronic structures are reported in the present work. The geometries of all the complexes under study were obtained with the *Gaussian 09* program package[29] at a scalar relativistic density functional theory (DFT) level. The PBE0[30,31] exchange-correlation functional is used, owing to its overall good performance for computing geometries of actinide complexes. The 60-electron small-core pseudopotentials ECP60MWB[32] were used to mimic the role of the core electrons of the An centers and implicitly introduce scalar relativistic effects, in conjunction with the (14s13p10d8f6g)/10s9p5d4f3g segmented basis sets[33]. The def2-TZVPD basis sets[34,35] are chosen for the O, N, C and H centers. The numerical grid was set according to the *grid = ultrafine* keyword of *Gaussian 09*. The nature of the stationary points was assessed by means of the computation of the vibrational frequencies, and the An oxidation states were assessed by analyzing the $<S^2>$ expectation values, the Mulliken atomic spin populations, and, to a lesser extent, the Mulliken atomic charges. Note that most of the oxidation states of the species of interest are obvious or were previously determined.[24] The Np oxidation state in $NpO_3(NO_3)_2^-$ was the only oxidation state that remained to be confirmed/attributed by calculations. This attribution was done by comparing the previously mentioned indicators to the ones obtained in the $NpO_2(NO_3)_3^-$ and $NpO_2(OH)(NO_3)_2^-$ cases, as well as by considering the equatorial Np−O vibrational frequency.

In previous work[24], we defined the magnetic coupling constant in $PuO_2(NO_3)_3^-$ at the high-spin geometry. This choice was made to unambiguously attribute the spin-doublet nature of the ground spin-orbit free state in this system. However, in the present work, we also compute gas-phase reaction energies. Although no ambiguity arose in the determination of the reactant energies in the $AnO_3(NO_3)_2^-$ (An = U, Np, Pu), $AnO_2(NO_3)_3^-$ (An = U, Np) and $AnO_2(OH)(NO_3)_2^-$ (An = U, Np, Pu) cases, the definition of a proper spin-orbit free energy for the $PuO_2(NO_3)_3^-$ complex deserves more attention. Due to antiferromagnetic coupling between the *S*=1 plutonyl unit and *S*=1/2 radical oxygen atom, the lowest energy solution that we previously reported correspond to a spin-broken-symmetry solution[24]. In order to assess the energy correction to be applied to the spin-broken-symmetry energy, we have used the approximate spin projection method,[36] at both the spin-broken-symmetry and high-spin geometries according to the following expression:

$$E_{\text{AP-BS}}^{\text{LS}} = \alpha E_{\text{U-BS}}^{\text{LS}} - \beta E_{\text{U}}^{\text{HS}}$$

where $E_{\text{AP-BS}}^{\text{LS}}$ is the corrected spin-broken symmetry energy, $E_{\text{U-BS}}^{\text{LS}}$ is the spin-unrestricted DFT spin-broken-symmetry energy, E_{U}^{HS} is the high-spin energy obtained with spin-unrestricted DFT, and α and β are defined as follows:

$$\alpha = \frac{\langle S^2 \rangle_{\text{U}}^{\text{HS}} - \langle S^2 \rangle_{\text{exact}}^{\text{LS}}}{\langle S^2 \rangle_{\text{U}}^{\text{HS}} - \langle S^2 \rangle_{\text{U-BS}}^{\text{LS}}}$$

and:

$$\beta = \frac{\langle S^2 \rangle_{\text{U-BS}}^{\text{LS}} - \langle S^2 \rangle_{\text{exact}}^{\text{LS}}}{\langle S^2 \rangle_{\text{U}}^{\text{HS}} - \langle S^2 \rangle_{\text{U-BS}}^{\text{LS}}}$$

where the $\langle S^2 \rangle$ expectation values are either the unrestricted DFT ones, or the ideal one for a pure low-spin state ("exact"), i.e. 0.75 for a $S = 1/2$ spin state.

Results and Discussion

Synthesis of $AnO_3(NO_3)_2^-$ complexes

The gas-phase $AnO_2(NO_3)_3^-$ complex ions (An = U, Np, Pu) were produced by ESI of solutions containing the actinyl cation, AnO_2^{2+}, and nitrate anion, NO_3^-. Full ESI mass spectra prior to ion isolation are shown in Figure S1. Before CID, all ions with other m/z were ejected from the QIT such that only the $AnO_2(NO_3)_3^-$ remained. The $AnO_2(NO_3)_3^-$ were then resonantly excited by applying a nominal CID voltage of 0.5 V, which results in multiple energetic collisions with the He bath gas. It should be noted that the CID "voltage" is an undefined instrumental parameter; the important point here is that the same excitation conditions were

applied to all the three $AnO_2(NO_3)_3^-$ complexes such that the fragmentation products and yields can be directly compared.

CID mass spectra for the three $AnO_2(NO_3)_3^-$ systems are shown in Figure 1. Comparison of the $AnO_2(NO_3)_3^-$ peak intensities in the parent ESI mass spectra (Figure S1) with the corresponding intensities in the CID mass spectra in Figure 1 reveals a much lower intensity in the latter. This decrease in intensity is due to substantial ion loss during isolation, which is particularly drastic in the negative ion mode. The dominant process in each case is reaction (2) to yield $AnO_3(NO_3)_2^-$. For An = Pu there is a minor product that corresponds to $PuO_2(NO_3)_2^-$, presumably $Pu^{V}O_2^+$ coordinated by two nitrate anion ligands. It should be noted that at higher CID voltages the product yields increase and additional minor products appear, as was previously reported for CID of $PuO_2(NO_3)_3^-$.[24] The lower energy CID conditions employed in the present study allow for comparison of the yields of the dominant $AnO_3(NO_2)_2^-$ products without substantial contributions from higher-energy fragmentation channels.

It is evident from Figure 1 that the CID yields of $UO_3(NO_3)_2^-$ and $PuO_3(NO_3)_2^-$ are essentially the same, with the CID $AnO_3(NO_3)_2^-$ product peaks having intensities of ~1/6 relative to the intact $AnO_2(NO_3)_3^-$ parent peaks; the fragmentation percentages are thus ~17% for both complexes. Under the same conditions, the CID yield of $NpO_3(NO_3)_2^-$ is contrastingly greater than the intensity of intact $NpO_2(NO_3)_3^-$, with an intensity ratio of ~28/17; for this complex the fragmentation percentage is ~160%. The comparative propensity for conversion of $AnO_2(NO_3)_3^-$ to $AnO_3(NO_3)_2^-$ is thus [(1/6)/(28/17)] ≈ 1/10 for $UO_2(NO_3)_3^-$ and $PuO_2(NO_3)_3^-$ versus $NpO_2(NO_3)_3^-$. The observation is that under the same conditions the unimolecular decomposition reaction (2) is about tenfold more efficient for An = Np versus An = U and Pu. This result indicates that reaction (2) is more favorable for $NpO_2(NO_3)_3^-$, in accord with computational results (vide infra). This can be taken to indicate a higher relative stability of the $NpO_3(NO_3)_2^-$ product compared with $UO_3(NO_3)_2^-$ and $PuO_3(NO_3)_2^-$. It was previously established that the oxidation state is Pu(VI) in the latter product and it can be assumed to be U(VI) in the uranium product, as this is obviously the terminal oxidation state. An obvious explanation for the more facile formation of $NpO_3(NO_3)_2^-$ is that the oxidation state is Np(VII) with a Np=O bond rather than a Np-O$^{\bullet}$ radical bond. This interpretation is substantiated by the computational and reactivity results presented below.

Computed structures and formation energies of $AnO_2(NO_3)_3^-$

The computed structures of the $AnO_2(NO_3)_3^-$ precursors and the $AnO_3(NO_3)_2^-$ CID products are shown in Figure 2. The geometries are similar for An = U, Np and Pu, except for a significant difference in one of the Np-O bond distances in the CID product. The bond distances identified in Figure 2 are given in Table 1. For the $AnO_2(NO_3)_3^-$ complexes, the distances **a** and **b** indicate actinyl(VI), AnO_2^{2+}, cores coordinated by three nitrate anion ligands. The bond distances are similar for the three $AnO_2(NO_3)_3^-$ complexes, with the actinide contraction resulting in slightly shorter distances from U to Np to Pu. The three $AnO_3(NO_3)_2^-$ can be considered as AnO_3^+ cores coordinated by two nitrate anion ligands. The distances **a´** and **b´** are

typical of actinyls coordinated by nitrates. The substantial discrepancy between the structures of the $AnO_3(NO_3)_2^-$ is apparent in the An-O bond distance **c**, which for An = Np is only slightly longer than the neptunyl distances but for An = U and Pu is substantially longer. The longer distance for An = Pu is consistent with previous results and the conclusion that the equatorial bond is a Pu-O$^{\bullet}$ radical bond; it is similarly concluded that the equatorial bond is a U-O$^{\bullet}$ radical bond with a U(VI) oxidation state. In the case of $NpO_3(NO_3)_2^-$ the much shorter equatorial bond distance **c** indicates a Np=O double bond, which corresponds to a Np(VII) oxidation state. Note that this bond distance, **c**, is significantly larger than the other two Np=O bonds (**a´**) that originate from the previous neptunyl unit, indicating that this "new" Np=O bond is not equivalent to the other two Np=O bonds and is weaker than them. The O_{ax}=An=O_{ax} actinyl bond angles in $UO_3(NO_3)_2^-$ and $PuO_3(NO_3)_2^-$ are close to linear (~178^o to 180^o), while there is a greater deviation in $NpO_3(NO_3)_2^-$ (~170°). The latter result is in accord with three somewhat similar three Np=O double bonds in $NpO_3(NO_3)_2^-$. This distortion of the O_{ax}=Np=O_{ax} bond angle is associated with changes in the O_{ax}=Np=O_{eq} bond angles, which are significantly larger than 90° in the Np complex, contrary to the O_{ax}=An-O_{eq} angles for the U and Pu complexes, which are very close to 90°.

The computed spin configurations for the $AnO_3(NO_3)_2^-$ complexes are doublet, singlet and doublet for An = U, Np and Pu, respectively. The doublet state for $UO_3(NO_3)_2^-$ is consistent with closed shell U(VI) (i.e., $5f^0$) and one unpaired electron on the radical O atom. Note that the obtained M_S = 1/2 solution in the An = Pu case corresponds to a mixture of spin-doublet and spin-quartet characters.[24] The doublet state for $PuO_3(NO_3)_2^-$ is consistent with two unpaired electrons on Pu(VI) (i.e., $5f^2$) antiferromagnetically coupled to the unpaired electron on the radical O. For assessing the geometry dependence of the energy correction to be applied to the energy of the spin-broken-symmetry solution, we computed this energy correction with the approximate spin projection method at both the spin-broken-symmetry and high-spin geometries. The corrections being −8 and −6 kJ/mol, respectively, we conclude that the correction is nearly independent of the geometry, and thus, use the spin-broken-symmetry geometry as our reference geometry for the discussion, while the computation of reaction energies will account for the approximate spin projection energy correction. In this way, we thus approximate the "true" spin-doublet geometry and energy without the need for using specific spin-broken-symmetry geometry optimization tools.[37] The singlet state for $NpO_3(NO_3)_2^-$ is consistent with closed-shell Np(VII) (i.e., $5f^0$) and a non-radical O atom (a closed-shell solution was found, i.e. $\langle S^2 \rangle$=0). Note that as in our previous work[24], all these interpretations of the spin patterns are supported by the analysis of atomic spin densities, and, to a lesser extent, by atomic charges.

An indicator of bond strength in actinyl complexes are the O=An=O vibrational frequencies, where higher frequencies indicate stronger bonds.[38,39] The computed frequencies for the $AnO_2(NO_3)_3^-$ and $AnO_3(NO_3)_2^-$ complexes are given in Table 2. The symmetric stretch ν_1 frequencies and asymmetric stretch ν_3 frequencies are all characteristic of AnO_2^{2+} moieties. The ν[An-O_{eq}] frequencies corresponding to the vibrational mode associated with the equatorial An-O bond are much lower for An = U and Pu, consistent with the assignment of these as having

single bond multiplicity character. The ν[An-O_{eq}] frequency, 774 cm^{-1}, is lower than but much closer to ν_1 and ν_3, consistent with the assignment of a higher (effective) bond order, close to two. This lower frequency compared with ν_1 and ν_3 indicates that the "new" Np=O bond is weaker than the two Np=O bonds in the $AnO_2(NO_3)_3^-$ complex.

The computed energies for the unimolecular dissociation reaction (2) are given in Table 3. The energy to eliminate NO_2 from $AnO_2(NO_3)_3^-$ for An = Np is lower, by 47 and 35 kJ/mol, than the energy for the corresponding An = U and Pu complexes, respectively. This result concurs with the experimental result of a greater CID yield of the $AnO_3(NO_3)_2^-$ complex for An = Np. As noted above, the higher stability of $NpO_3(NO_3)_2^-$ is in accord with formation of a stable gas-phase Np(VII) complex, as is indicated by the other experimental and computational results.

Reactions with the $AnO_3(NO_3)_2^-$ complexes

Two reactions involving the $AnO_3(NO_3)_2^-$ systems were studied under thermal condition in the QIT to identify differences in chemistry and evaluate disparities from the perspective of the structures and bonding in the anion complexes. Reaction (3) is the reverse of the endothermic CID reaction (2).

$$AnO_3(NO_3)_2^- + NO_2 \rightarrow An^{VI}O_2(NO_3)_3^- \qquad (3)$$

For reaction (3) to occur spontaneously under thermal conditions it must be exothermic and have no prohibitive energy barrier above the reactants on the potential energy surface, as has been discussed for the dissociative insertion of CO_2 into $NUOCl_2^-$.[40] The results in Figure 3 demonstrate that reaction (3) occurs for An = U and Pu, but not for An = Np to within the experimental detection limit. Taking into consideration the different reaction times, the following comparative efficiencies for reaction (3) are obtained, arbitrarily normalized to a value of 100 for uranium: $UO_3(NO_3)_2^-$ / 100 > $PuO_3(NO_3)_2^-$ / 5 >> $NpO_3(NO_3)_2^-$ / <0.02 (product not detected). The very disparate reaction efficiencies, notably that reaction (3) is at least 5000 more efficient for An = U versus An = Np, evidently reflects very different susceptibilities of U-$O^{\bullet}$ and Np=O bonds towards activation. A greater reactivity of the uranium complex would be expected due to the radical equatorial oxygen. In contrast, all three neptunium-oxygen bonds in the reactant are double bonds and there is thus no oxygen atom that should be so highly reactive, as is required for formation of a NO_3 anion ligand upon addition of NO_2. Although reaction (3) spontaneously occurs for $PuO_3(NO_3)_2^-$ it does so with an efficiency ~20 times lower than for the uranium complex. The reason for this reduced reactivity is not readily apparent from the computed structures, which are similar and feature U-$O^{\bullet}$ and Pu-$O^{\bullet}$ bonds; there are clearly other factors that affect the reaction kinetics, as discussed below. The key finding is that, in contrast to the uranium and plutonium complexes, reaction (3) is not detected for $NpO_3(NO_3)_2^-$, which is thus at least 250 times less reactive than $PuO_3(NO_3)_2^-$. This result is consistent with the computed structures: radical Pu-$O^{\bullet}$ versus saturated Np=O.

The computed energetics for reaction (3), which are simply the inverse of those for endothermic CID reaction (2), are in Table 3. Compared with An = U, reaction (3) is slightly less exothermic for An = Pu and significantly less exothermic for An = Np. These energetics are in accord with the observed reactivity, U > Pu >> Np. It should be emphasized that although there is generally a correlation between reaction rates and thermodynamics for similar reaction mechanisms, the kinetics are determined by the reaction energy profiles, specifically by transition state barriers thereon, and not necessarily by the overall reaction energetics.[41] The higher yield of $NpO_3(NO_3)_2^-$ was attributed to a stable Np(VII) complex with a Np=O equatorial bond; the comparatively higher resistance of this complex to react with NO_2 to revert to $NpO_2(NO_3)_3^-$ is similarly attributed to the lesser propensity for reduction of Np(VII) to Np(VI).

A notable result is that reaction (3) is about 20 times less efficient for An = Pu versus An = U. Although this disparity is not as large as for An = Pu versus An = Np, it is nonetheless significant. The magnitudes of the reaction exothermicities, U > Pu > Np, are in parallel with the observed reaction rates. The lesser reactivity of $PuO_3(NO_3)_2^-$ versus $UO_3(NO_3)_2^-$ may be related to the accessibility of Pu(VII) but not U(VII)—it is possible that the Pu complex exhibits some Pu(VII) character that is not readily apparent from the structures, but is manifested in both the observed reactivities and the computed reaction energetics.

Reaction (4) was also studied for the three $AnO_3(NO_3)_2^-$ complexes, where $C_6H_5CH_3$ is toluene (methyl benzene; deuterated $C_6D_5CD_3$ was employed in the experiments).

$$AnO_3(NO_3)_2^- + C_6H_5CH_3 \rightarrow AnO_2(OH)(NO_3)_2^- + C_6H_5CH_2 \qquad (4)$$

Toluene was used as a hydrogen atom donor because of its relatively low C-H bond dissociation energy, $D[C_6H_5CH_2\text{-}H]$ = 389 kJ/mol, which is substantially lower than, for example, D[HO-H] = 497 kJ/mol for water.[42] The results for reaction (4) are shown in Figure 4. Because $C_6D_5CD_3$ was used for the experiments the product of reaction (4) should be $AnO_2(OD)(NO_3)_2^-$at 2 m/z above the reactant. Although the $UO_3(NO_3)_2^-$ complex exhibits reactivity, the dominant product is $UO_2(OH)(NO_3)_2^-$ at 1 m/z above the reactant, with only a minor yield of $UO_2(OD)(NO_3)_2^-$. This is attributed to facile exchange with background water in the ion trap, as given by reaction (5).

$$UO_2(OD)(NO_3)_2^- + H_2O \rightarrow UO_2(OH)(NO_3)_2^- + D_2O \qquad (5)$$

Evidence for this exchange reaction is presented in Figure 5. The minor yield of $UO_2(OD)(NO_3)_2^-$ produced during CID was isolated and allowed to react with background water in the ion trap for 250 ms, after which approximately 50% of the OD had been replaced by OH. The results shown in Figure 4 were for a much longer reaction time, 10 s, such that most of the OD would be replaced by OH. In Figure 4, the spectra on the right hand side correspond to the same reaction conditions except with an increase in the pressure of $C_6D_5CD_3$. For high pressures

of $C_6D_5CD_3$, or any reagent gas, the performance of the ion trap deteriorates, which is apparent as a substantial decrease in ion intensity, even in the absence of a reaction.

The results in Figure 4 demonstrate that reaction (4) is observed for An = U, but not for An = Np or Pu. The peak at 415 m/z in the mass spectrum for reaction of $PuO_3(NO_3)_2^-$ with toluene at the higher pressure (Figure 4c, spectrum on right) corresponds to $PuO_2(OH)(NO_3)_2^-$, but the very low absolute intensity renders this apparent minor reactivity results as inconclusive. Assigning the minuscule peak at 415 m/z as the experimental detection limit, it is concluded that with toluene both $NpO_3(NO_3)_2^-$ and $PuO_3(NO_3)_2^-$ are both at least 500 times less reactive than $UO_3(NO_3)_2^-$.

It should be noted that $UO_3(NO_3)_2^-$ exhibits some reactivity with background gases in the ion trap. From Figure S2 it is apparent that the intensity of the $UO_2(OH)(NO_3)_2^-$ product peak is ca. 15% of the intensity of the $UO_3(NO_3)_2^-$ peak after 10 s reaction with background gases in the trap. Although the source of hydrogen atoms is not known, water is excluded because abstraction of an H atom from H_2O by $UO_3(NO_3)_2^-$ is computed to be endothermic by ~30 kJ/mol. Neither $NpO_3(NO_3)_2^-$ nor $PuO_3(NO_3)_2^-$ exhibited detectable reactivity with background gases in the ion trap (Figure S2). In parallel with the results for the reactions with toluene, it is apparent from reaction with indeterminate background gases that $UO_3(NO_3)_2^-$ is much more efficient at H-atom abstraction than are the corresponding Np and Pu complexes.

The computed structures for the $AnO_2(OH)(NO_3)_2^-$ products of reaction (4) are shown in Figure S3 (geometrical parameters are given in Table S1). These are An(VI) anion complexes having an actinyl(VI) moiety coordinated in the equatorial plane by two nitrate ligands and one hydroxide ligand. The computed energies for reaction (4) are in Table 3. Although the reaction is predicted to be exothermic for all three $AnO_3(NO_3)_2^-$, it is moderately (by 16 kJ/mol) more so for An = U versus An = Pu, and significantly more so (by 24 kJ/mol) for An = Pu versus An = Np. These comparative energetics closely parallel those for reaction (3). The result that among the three $AnO_3(NO_3)_2^-$ complexes, reactivity with toluene is observed only for An = U reinforces the conclusion that this complex can be characterized as distinctly U(VI). Although both the uranium and plutonium complexes have An-O$^\bullet$ radical bonds and formal oxidation states of An(VI) it would appear that the Pu-O$^\bullet$ bond is less susceptible towards activation, particularly conversion to a Pu-OH moiety, than is the U-O$^\bullet$ bond. The overall reactivity results suggest some higher oxidation state character in the case of $PuO_3(NO_3)_2^-$, and Np(VII) in $NpO_3(NO_3)_2^-$. The difference between $UO_3(NO_3)_2^-$ and $PuO_3(NO_3)_2^-$, notably the apparently greater stability of the latter that may be due to an accessible Pu(VII) oxidation state, is not readily apparent from the very similar structures of the two complexes. The experimental observations suggest that whereas it is a distinct single U-O$^\bullet$ bond, there may be some partial character of a higher bond multiplicity in the "Pu-O$^\bullet$" moiety.

The different bonding properties in the An-O_{eq} bonds thus appear related to the potential involvement in a further chemical bond of the non-bonding electrons of the AnO_2^{2+} core in the $AnO_2(NO_3)_3^-$ complex. In the case of An=U, the absence of non-bonding electrons in this core prevents the formation of a further U=O double bond. In the case of An = Np, the presence of

one non-bonding electron in this core, that is furthermore relatively easy to engage in a chemical bond or even withdraw, as indicated by a relatively low Np(VII/VI) reduction potential, leads to the formation of a further Np=O double bond, and thus to Np(VII). In the case of An = Pu, two non-bonding electrons are present in this core; it is however harder to engage one of them in a chemical bond, as indicated by a somewhat higher Pu(VII/VI) reduction potential, with the result that Pu is not further oxidized and only a single Pu-O$^{\bullet}$ multiple radical bond is formed.

Summary and Conclusions

Gas-phase actinyl(VI) nitrate anion complexes, $AnO_2(NO_3)_3^-$ (An = U, Np, Pu), were produced by ESI of actinyl nitrate solutions. Energetic CID fragmentation of these complexes results in elimination of NO_2 to yield $AnO_3(NO_3)_2^-$. In the AnO_3^+ core of these anion products the actinide oxidation state is conceivably An(VII). The higher yield of $NpO_3(NO_3)_2^-$ suggests that the oxidation state is Np(VII) whereas it is An(VI) in the U and Pu complexes. Computed structures and spin configurations are in accord with this interpretation. The NpO_3^+ core can be considered as neptunyl with an equatorial Np=O double bond, whereas the UO_3^+ and PuO_3^+ cores are actinyls, each of them with an equatorial An-O$^{\bullet}$ bond. The result that radical O$^{\bullet}$ oxidizes Np(VI) but not Pu(VI) is in accord with the higher reduction potential for Pu(VII/VI) versus Np(VII/VI). As expected, it is impractical to attain the U(VII) oxidation state.

Whereas $UO_3(NO_3)_2^-$ and $PuO_3(NO_3)_2^-$ spontaneously chemisorb NO_2 to regenerate the stable actinyl(VI) nitrate complexes, $NpO_3(NO_3)_2^-$ does not, in accord with the assignment of the latter as a stable Np(VII) complex. Computed energetics for NO_2 chemisorptions parallel observed reactivities, with the energy for the Np complex being the least favorable. The reactions of $AnO_3(NO_3)_2^-$ with toluene, an effective H-atom donor, are predicted to exothermically yield $AnO_2(OH)(NO_3)_2^-$ for An = U, Np and Pu. The H-atom abstraction reaction is observed for An = U, but not for An = Np and Pu; the computed energetics are most favorable for An = U and least so for An = Np. These observed reactivities and computed energetics suggest that in the $AnO_3(NO_3)_2^-$ complexes the oxidation states are distinctly U(VI) and Np(VII). In $PuO_3(NO_3)_2^-$, it may be primarily Pu(VI) with some contribution from Pu(VII).

A particularly significant result is the attainment of an elementary gas-phase species containing Np(VII). This reveals that heptavalent Np can be prepared absent stabilizing effects in condensed phase environments. The results indicate that in AnO_3^+ a radical O$^{\bullet}$ atom oxidizes Np(VI) to Np(VII) but not Pu(VI) to Pu(VII), in accord with the higher Pu(VII/VI) versus Np(VII/VI) reduction potential. This is a case of the nature of elementary gas-phase complexes revealing fundamental actinide chemistry.

Supplemental Information

ESI mass spectra for the uranyl, neptunyl and plutonyl nitrate solutions. Mass spectra acquired after reactions of $AnO_3(NO_3)_2^-$ with background gases in the ion trap. Computed structures and geometrical parameters of the $AnO_2(OH)(NO_3)_2^-$ complexes.

Acknowledgements

The work of P.D.D. and J.K.G. was fully supported by the U.S. Department of Energy, Office of Basic Energy Sciences, Heavy Element Chemistry, at LBNL under Contract No. DE-AC02-05CH11231. Calculations were carried out using HPC resources from GENCI-CINES/IDRIS (grant 2015-c2015085117) and CCIPL ("Centre de Calcul Intensif des Pays de la Loire").

References

(1) Spitsyn, V. I.; Gelman, A. D.; Krot, N. N.; Mefodiye.Mp; Zakharov.Fa; Komkov, Y. A.; Shilov, V. P.; Smirnova, I. V. Heptavalent State of Neptunium and Plutonium. *J. Inorg. Nucl. Chem.* **1969**, *31*, 2733-2745.

(2) Clark, D. L.; Conradson, S. D.; Neu, M. P.; Palmer, P. D.; Runde, W.; Tait, C. D. XAFS Structural Determination of Np(VII). Evidence for a Trans Dioxo Cation Under Alkaline Solution Conditions. *J. Am. Chem. Soc.* **1997**, *119*, 5259-5260.

(3) Gogolev, A. V.; Fedosseev, A. M.; Moisy, P. The Influence of F-Elements' Oxidizing Potential and Ion Charge on their Stability in Aqueous Alkaline Solution. *Radiochim. Acta* **2012**, *100*, 809-811.

(4) Williams, C. W.; Blaudeau, J. P.; Sullivan, J. C.; Antonio, M. R.; Bursten, B.; Soderholm, L. The Coordination Geometry of Np(VII) in Alkaline Solution. *J. Am. Chem. Soc.* **2001**, *123*, 4346-4347.

(5) Bolvin, H.; Wahlgren, U.; Moll, H.; Reich, T.; Geipel, G.; Fanghanel, T.; Grenthe, I. On the Structure of Np(VI) and Np(VII) Species in Alkaline Solution Studied by EXAFS and Quantum Chemical Methods. *J. Phys. Chem. A* **2001**, *105*, 11441-11445.

(6) Bratsch, S. G. Standard Electrode-Potentials and Temperature Coefficients in Water at 298.15 K. *J. Phys. Chem. Ref. Data* **1989**, *18*, 1-21.

(7) Sullivan, J. C.; Zielen, A. J. Oxidation of Water by Np(VII) in Aqueous Perchloric Acid Media. *Inorg. Nucl. Chem. Lett.* **1969**, *5*, 927-931.

(8) Keller, C.; Seiffert, H. Li5NpO6,First Crystalline Compound with Heptavalent Neptunium and Existence of Heptavalent Plutonium and Americium. *Inorg. Nucl. Chem. Lett.* **1969**, *5*, 51-57.

(9) Burns, J. H.; Baldwin, W. H.; Stokely, J. R. Studies with Heptavalent Neptunium - Identification and Crystal-Structure Analysis of LiCo(NH3)6Np2O8(OH).2(2H2O). *Inorg. Chem.* **1973**, *12*, 466-469.

(10) Grigoriev, M. S.; Krot, N. N. Novel Heptavalent Actinide Compounds: Tetrasodium Dihydroxidotetraoxidoneptunate(VII) Hydroxide Dihydrate and its Plutonium Analogue. *Acta Crystallogr. C* **2009**, *65*, I91-I93.

(11) Smith, A. L.; Raison, P. E.; Konings, R. J. M. Synthesis and Crystal Structure Characterisation of Sodium Neptunate Compounds. *J. Nucl. Mater.* **2011**, *413*, 114-121.

(12) Kiselev, Y. M.; Nikonov, M. V.; Tananaev, I. G.; Myasoedov, B. F. On the Existence of Plutonium Tetroxide. *Dokl. Phys. Chem.* **2009**, *425*, 73-76.

(13) Kiselev, Y. M.; Nikonov, V. M.; Dolzhenko, V. D.; Ermilov, A. Y.; Tananaev, I. G.; Myasoedov, B. F. Spectroscopic Study of Plutonium Tetroxide. *Dokl. Chem.* **2009**, *426*, 91-95.

(14) Nikonov, M. V.; Kiselev, Y. M.; Tananaev, I. G.; Myasoedov, B. F. Plutonium Volatility in Ozonization of Alkaline Solutions of Pu(VI) Hydroxo Complexes. *Dokl. Chem.* **2011**, *437*, 69-71.

(15) Huang, W.; Xu, W. H.; Su, J.; Schwarz, W. H. E.; Li, J. Oxidation States, Geometries, and Electronic Structures of Plutonium Tetroxide PuO_4 Isomers: Is Octavalent Pu Viable? *Inorg. Chem.* **2013**, *52*, 14237-14245.

(16) Huang, W.; Pyykko, P.; Li, J. Is Octavalent Pu(VIII) Possible? Mapping the Plutonium Oxyfluoride Series PuO_nF_{8-2n} (n=0-4). *Inorg. Chem.* **2015**, *54*, 8825-8831.

(17) Fargeas, M.; Fremontlamouranne, R.; Legoux, Y.; Merini, J. Actinide Fluorides and Oxyfluorides with High Valencies, Studied Using Thermochromatography. *J. Less-Common Met.* **1986**, *121*, 439-444.

(18) Albury, R. M.; Pruitt, C. J. M.; Hester, T. H.; Goebbert, D. J. Fragmentation of Cr(NO3)(4)(-): Metal Oxidation upon $O^{\bullet-}$ Abstraction. *J. Phys. Chem. A* **2015**, *119*, 11471-11478.

(19) Pruitt, C. J. M.; Goebbert, D. J. Experimental and Theoretical Study of the Decomposition of Copper Nitrate Cluster Anions. *J. Phys. Chem. A* **2015**, *119*, 4755-4762.

(20) Li, F. M.; Byers, M. A.; Houk, R. S. Tandem Mass Spectrometry of Metal Nitrate Negative Ions Produced by Electrospray Ionization. *J. Am. Soc. Mass Spectr.* **2003**, *14*, 671-679.

(21) Schröder, D.; Holthausen, M. C.; Schwarz, H. Radical-Like Activation of Alkanes by the Ligated Copper Oxide Cation (Phenanthroline)CuO. *J. Phys. Chem. B* **2004**, *108*, 14407-14416.

(22) Franski, R.; Sobieszczuk, K.; Gierczyk, B. Mass Spectrometric Decomposition of $[M^{n+}(NO3^{-})_{n+1}]^{-}$ Anions Originating from Metal Nitrates $M(NO3)_n$. *Int. J. Mass. Spectrom.* **2014**, *369*, 98-104.

(23) Lucena, A. F.; Lourenço, C.; Michelini, M. C.; Rutkowski, P. X.; Carretas, J. M.; Zorz, N.; Berthon, L.; Dias, A.; Oliveira, M. C.; Gibson, J. K.; Marçalo, J. Synthesis and Hydrolysis of Gas-Phase Lanthanide and Actinide Oxide Nitrate Complexes: A Correspondence to Trivalent Metal Ion Redox Potentials and Ionization Energies. *Phys. Chem. Chem. Phys.* **2015**, *17*, 9942-9950.

(24) Maurice, R.; Renault, E.; Gong, Y.; Rutkowski, P. X.; Gibson, J. K. Synthesis and Structures of Plutonyl Nitrate Complexes: Is Plutonium Heptavalent in PuO3(NO3)(2)(-) ? *Inorg. Chem.* **2015**, *54*, 2367-2373.

(25) Rios, D.; Rutkowski, P. X.; Shuh, D. K.; Bray, T. H.; Gibson, J. K.; Van Stipdonk, M. J. Electron Transfer Dissociation of Dipositive Uranyl and Plutonyl Coordination Complexes. *J. Mass Spectrom.* **2011**, *46*, 1247-1254.

(26) Gronert, S. Estimation of Effective Ion Temperatures in a Quadrupole Ion Trap. *J. Am. Soc. Mass Spectr.* **1998**, *9*, 845-848.

(27) Rutkowski, P. X.; Michelini, M. C.; Bray, T. H.; Russo, N.; Marçalo, J.; Gibson, J. K. Hydration of gas-phase ytterbium ion complexes studied by experiment and theory. *Theor. Chem. Acc.* **2011**, *129*, 575-592.

(28) Rios, D.; Michelini, M. C.; Lucena, A. F.; Marçalo, J.; Bray, T. H.; Gibson, J. K. Gas-Phase Uranyl, Neptunyl, and Plutonyl: Hydration and Oxidation Studied by Experiment and Theory. *Inorg. Chem.* **2012**, *51*, 6603-6614.

(29) Frisch, M. J.*; et al.* Gaussian 2009 (revision D.01). See Supporting Information for full citation.

(30) Perdew, J. P.; Emzerhof, M.; Burke, K. Rationale for mixing exact exchange with density functional approximations. *J. Chem. Phys.* **1996**, *105*, 9982-9985.

(31) Adamo, C.; Barone, V. Toward reliable density functional methods without adjustable parameters: The PBE0 model. *J. Chem. Phys.* **1999**, *110*, 6158-6170.

(32) Cao, X. Y.; Dolg, M.; Stoll, H. Valence basis sets for relativistic energy-consistent small-core actinide pseudopotentials. *J. Chem. Phys.* **2003**, *118*, 487-496.

(33) Cao, X.; Dolg, M. Segmented contraction scheme for small-core actinide pseudopotential basis sets. *J. Molec. Struct. (THEOCHEM)* **2004**, *673*, 203-209.

(34) Weigend, F.; Ahlrichs, R. Balanced basis sets of split valence, triple zeta valence and quadruple zeta valence quality for H to Rn: Design and assessment of accuracy. *Phys. Chem. Chem. Phys.* **2005**, *7*, 3297-3305.

(35) Rappoport, D.; Furche, F. Property-optimized Gaussian basis sets for molecular response calculations. *J. Chem. Phys.* **2010**, *133*.

(36) Kitagawa, Y.; Saito, T.; Nakanishi, Y.; Kataoka, Y.; Matsui, T.; Kawakami, T.; Okumura, M.; Yamaguchi, K. Spin Contamination Error in Optimized Geometry of Singlet Carbene ((1)A(1)) by Broken-Symmetry Method. *J. Phys. Chem. A* **2009**, *113*, 15041-15046.

(37) Saito, T.; Kitagawa, Y.; Shoji, M.; Nakanishi, Y.; Ito, M.; Kawakami, T.; Okumura, M.; Yamaguchi, K. Theoretical studies on the structure and effective exchange integral (J(ab)) of an active site in oxyhemocyanin (oxyHc) by using approximately spin-projected geometry optimization (AP-opt) method. *Chem. Phys. Lett.* **2008**, *456*, 76-79.

(38) Groenewold, G. S.; Gianotto, A. K.; Cossel, K. C.; Van Stipdonk, M. J.; Moore, D. T.; Polfer, N.; Oomens, J.; de Jong, W. A.; Visscher, L. Vibrational Spectroscopy of Mass-Selected [UO2(ligand)(n)](2+) Complexes in the Gas Phase: Comparison with Theory. *J. Am. Chem. Soc.* **2006**, *128*, 4802-4813.

(39) Gibson, J. K.; Hu, H. S.; Van Stipdonk, M. J.; Berden, G.; Oomens, J.; Li, J. Infrared Multiphoton Dissociation Spectroscopy of a Gas-Phase Complex of Uranyl and 3-Oxa-Glutaramide: An Extreme Red-Shift of the [O=U=O](2+) Asymmetric Stretch. *J. Phys. Chem. A* **2015**, *119*, 3366-3374.

(40) Dau, P. D.; Armentrout, P. B.; Michelini, M. C.; Gibson, J. K. Activation of Carbon Dioxide by a Terminal Uranium-Nitrogen Bond in the Gas-Phase: A Demonstration of the Principle of Microscopic Reversibility. *Phys. Chem. Chem. Phys.* **2016**, *18*, 7334-7340.

(41) Rios, D.; Michelini, M. D.; Lucena, A. F.; Marçalo, J.; Gibson, J. K. On the Origins of Faster Oxo Exchange for Uranyl(V) versus Plutonyl(V). *J. Am. Chem. Soc.* **2012**, *134*, 15488-15496.

(42) Lias, S. G.; Bartmess, J. E.; Liebman, J. F.; Holmes, J. L.; Levin, R. D.; Mallard, W. G. Gas-Phase Ion and Neutral Thermochemistry. *J. Phys. Chem. Ref. Data* **1988**, *17*, 1-861.

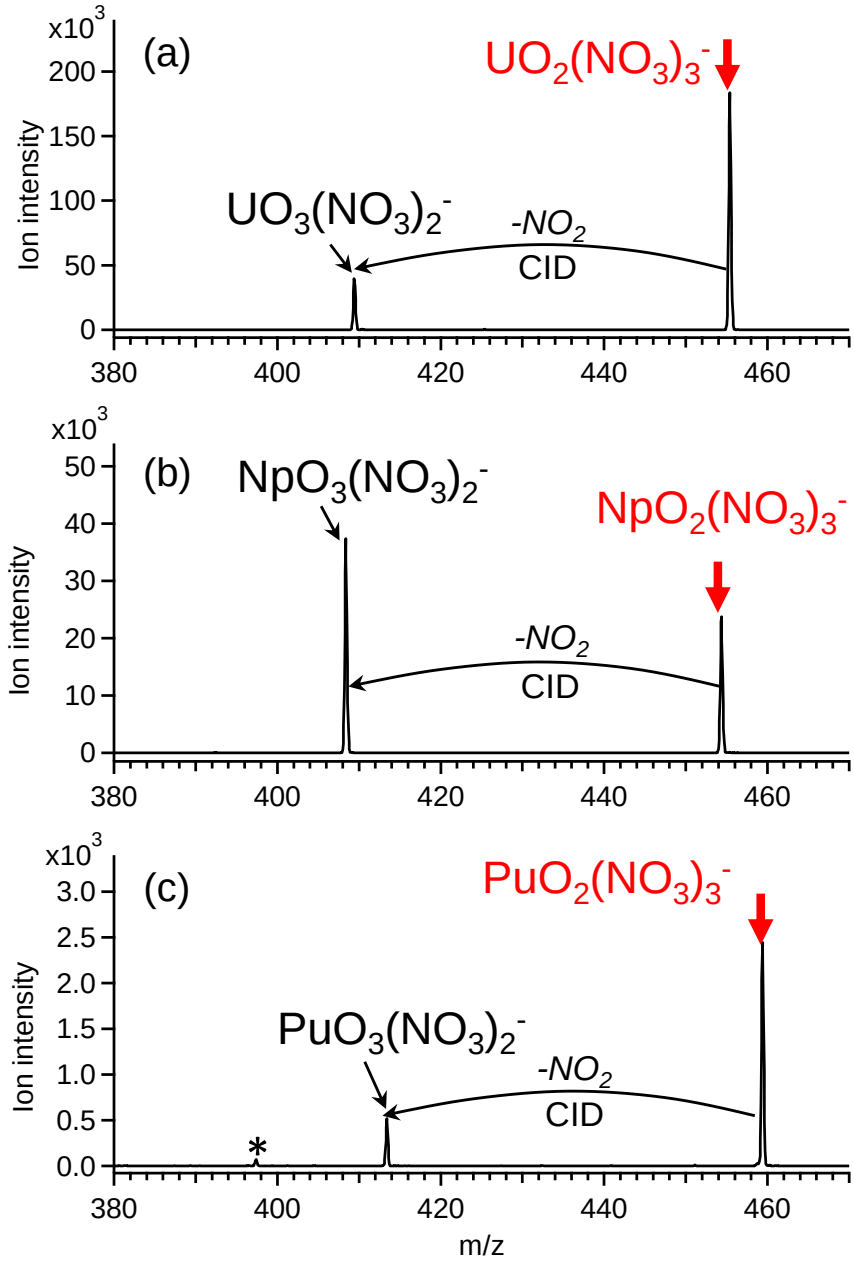

Figure 1. Mass spectra for CID of the three $AnO_2(NO_3)_3^-$ complexes indicated in red: (a) An = U; (b) An = Np; (c) An = Pu. The three spectra were acquired under the same conditions. In all cases the dominant product is $AnO_3(NO_3)_2^-$ from reaction (2). The minor peak identified with an asterisk in (c) corresponds to $PuO_2(NO_3)_2^-$. No other significant peaks appeared in the CID spectra.

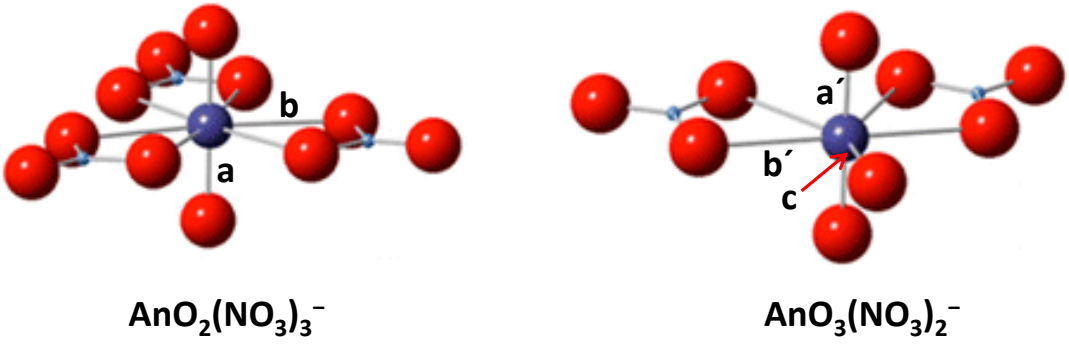

$AnO_2(NO_3)_3^-$ $AnO_3(NO_3)_2^-$

Figure 2. Computed structures of $AnO_2(NO_3)_3^-$ and $AnO_3(NO_3)_2^-$ (An = U, Np, Pu). The bond distances a, b, a´, b´ and c are given in Table 1.

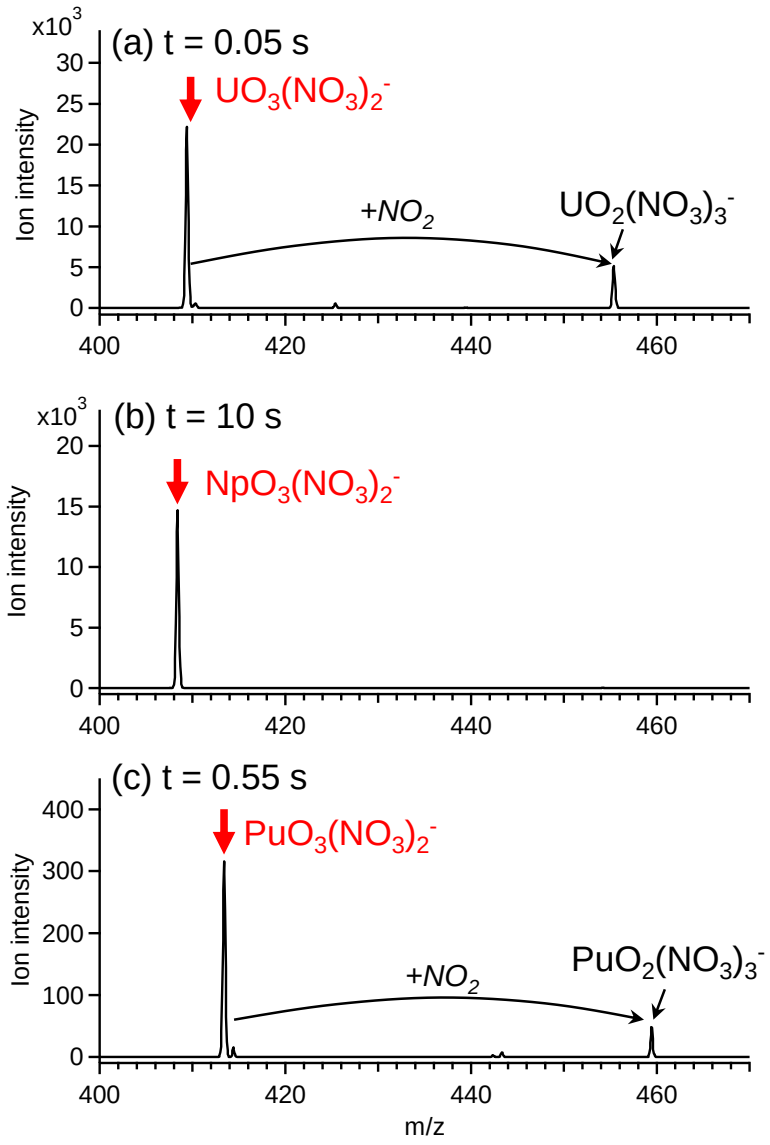

Figure 3. Mass spectra acquired after reaction of isolated $AnO_3(NO_3)_2^-$ indicated in red with NO_2 at the same pressure but different reaction time t: (a) An = U, t = 0.05 s; (b) An = Np, t = 10 s; (c) An = Pu, t = 0.55 s. The product of reaction (3) is apparent in (a) and (c) but not (b). The minor peaks at 1 m/z higher than the reactant peaks in (a) and (c) are assigned as $AnO_2(OH)(NO_3)_2^-$; the source of the H atoms is indeterminate but could be HNO_2, which is a facile H-atom donor.

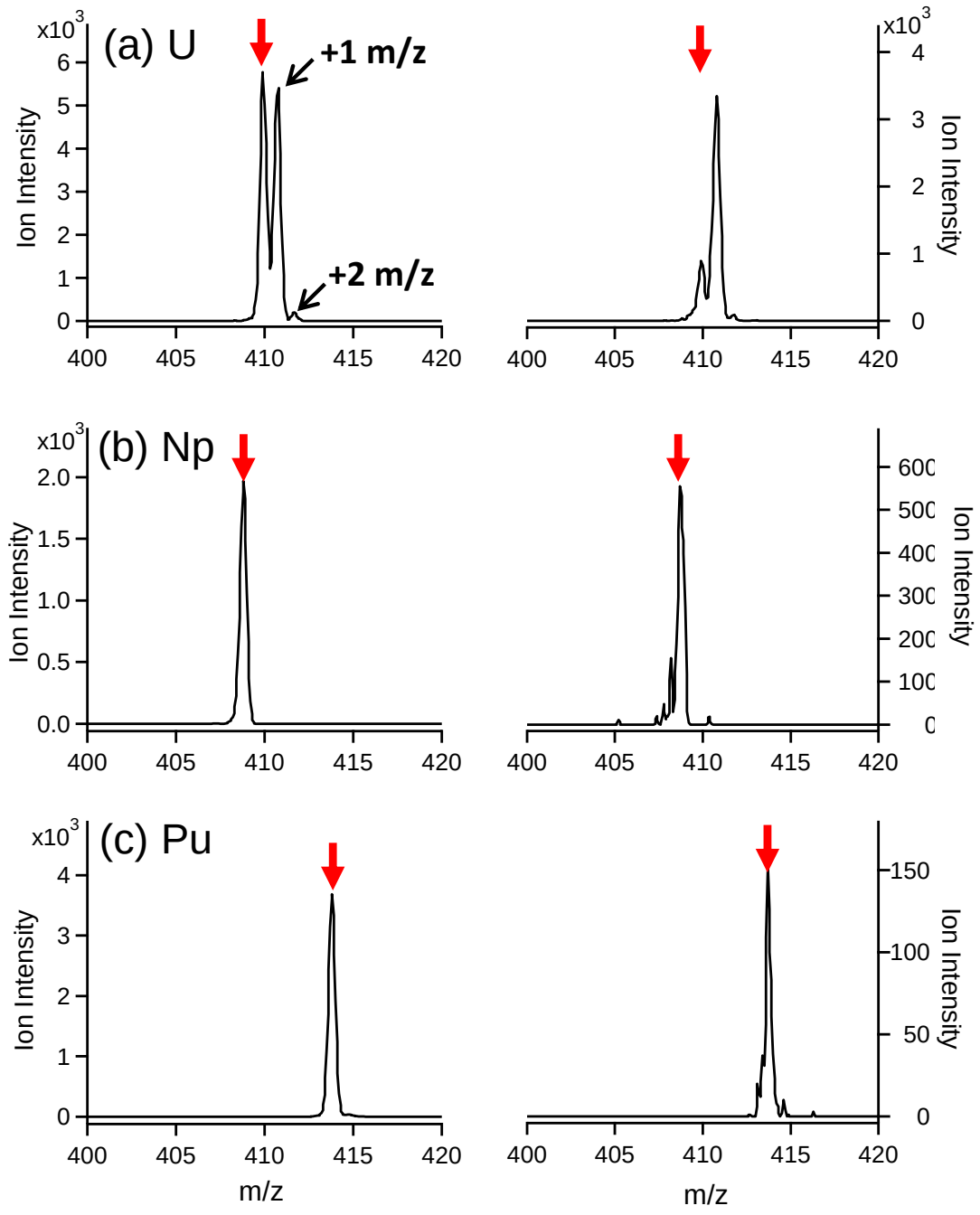

Figure 4. Mass spectra acquired after a 10 s reaction time of isolated $AnO_3(NO_3)_2^-$ denoted by red arrows with deuterated toluene ($C_6D_5CD_3$) at a lower (left spectra) and higher (right spectra) reagent pressure: (a) $UO_3(NO_3)_2^-$; $NpO_3(NO_3)_2^-$; $PuO_3(NO_3)_2^-$. Only $UO_3(NO_3)_2^-$ abstracts a D-atom to yield $UO_2(OD)(NO_3)_2^-$ (+2 m/z); this primary product rapidly exchanges with background H_2O in the ion trap to yield the dominant $UO_2(OH)(NO_3)_2^-$ (+1 m/z) ultimate product.

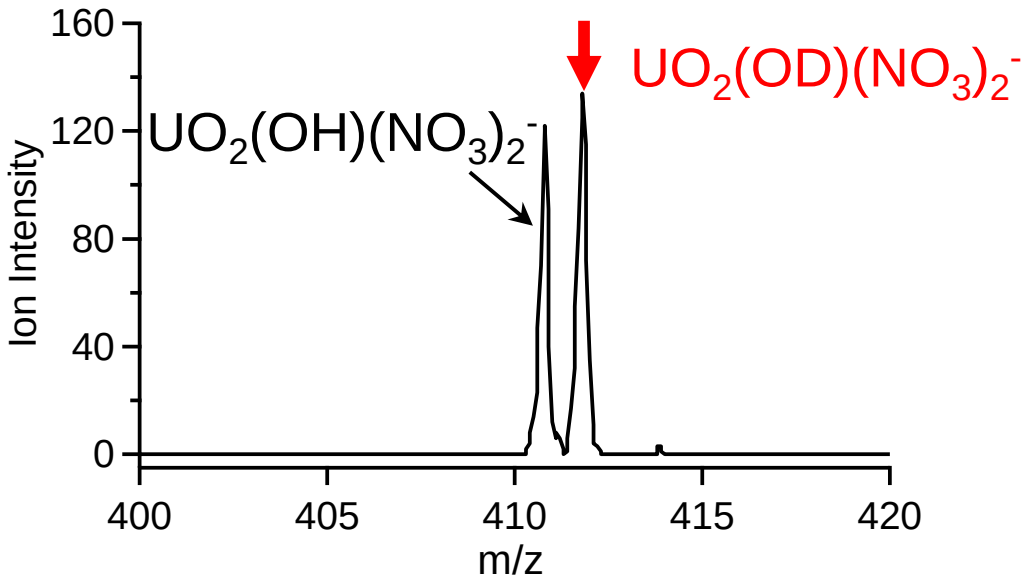

Figure 5. Mass spectra acquired after a 250 ms reaction time of isolated $UO_2(OD)(NO_3)_2^-$ (red arrow) produced without applying a delay. The $C_6D_5CD_3$ pressure is the same as for the low-pressure spectra in Fig. 4. The conversion of $UO_2(OD)(NO_3)_2^-$ to $UO_2(OH)(NO_3)_2^-$ reveals that exchange with background H_2O in the ion trap occurs on a faster time scale than D-abstraction from $C_6D_5CD_3$.

Table 1. Computed bond distances (Å) for the complexes in Figure 2.

	$AnO_2(NO_3)_3^-$		$AnO_3(NO_3)_2^-$		
	a	**b**	**a´**	**b´**	**c**
U	1.75	2.48	1.76	2.48−2.53	2.12
Np	1.74	2.46	1.74	2.47−2.51	1.82
Pu[a]	1.71	2.46	1.72	2.47−2.51	2.08

[a] Taken from reference 24.

Table 2. Computed An-O vibrational frequencies (cm^{-1})[a]

	$AnO_2(NO_3)_3^-$		$AnO_3(NO_3)_2^-$		
	ν_1	ν_3	ν_1	ν_3	ν[An-O_{eq}]
U	924	996	901	967	463
Np	917	1007	904	966	774
Pu	906	1014	885	984	432

[a] ν_1 and ν_3 are the actinyl O=An=O symmetric and asymmetric modes, respectively. ν[An-O_{eq}] is the frequency of the equatorial An-O (Np=O) vibrational mode.

Table 3. Computed energies (kJ/mol) for reactions (2), (3) and (4).

	U	**Np**	**Pu**
Reaction (2) *$AnO_3(NO_3)_2^-$ from $AnO_2(NO_3)_3^-$*	294	247	282
Reaction (3)[a] *Addition of NO_2 to $AnO_3(NO_3)_2^-$*	−294	−247	−282
Reaction (4) *H-abstraction from $C_6H_5CH_3$*	−86	−46	−70

[a] These are simply the opposite of reaction (2) energies.

TOC Graphic

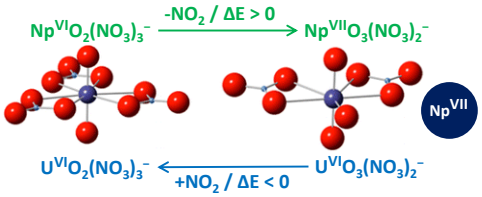

The heptavalent oxidation state of neptunium has been achieved in a gas-phase coordination complex. $AnO_3(NO_3)_2^-$ (An = U, Np, Pu) are nitrate-coordinated AnO_3^+ cores. Addition of NO_2 to yield $An^{VI}O_2(NO_3)_3^-$ indicates U^{VI} and Pu^{VI} in AnO_3^+, with An-$O^{\bullet}$ radical bonds. Contrastingly inert character of $NpO_3(NO_3)_2^-$ supports computations showing Np^{VII} in the NpO_3^+ core. Oxidation of Np^{VI} but not Pu^{VI} by an $O^{\bullet}$ radical indicates intrinsically greater stability of Np^{VII} versus Pu^{VII}.